

Tapered Quantum Cascade Lasers in the long-wavelength mid infrared region

Davide Pinto^{*a,b}, Kumar Kinjalk^b, Ariane Meguekam^b, Michael Bahriz^b, Alexei N. Baranov^b
^aInstitute of Chemical Technologies and Analytics, TU Wien, Getreidemarkt 9/164, 1060 Vienna, Austria

^bInstitute of Electronics and Systems, UMR 5214 CNRS University of Montpellier, 34095 Montpellier, France

ABSTRACT

We present an investigation on the electrical and optical properties of tapered quantum cascade lasers emitting at 14-15 μm , based on the InAs/AlSb system. In tapered lasers the active zone volume is increased to obtain higher optical power outputs without degrading the beam quality. Devices with three different taper angles of 1°, 2° and 3° were examined in terms of electrical, optical, and spectral properties and were compared with conventional ridge waveguide lasers.

Keywords: Quantum Cascade Laser, Tapered lasers, long-wavelength infrared, small slow-axis divergence

1. INTRODUCTION

Quantum cascade lasers (QCLs) have proven to be a versatile source of mid-infrared coherent radiation. QCLs based on the InAs/AlSb system, often called antimonide lasers, can be engineered to emit in the long-wavelength (LW) infrared range ($\lambda > 10 \mu\text{m}$). The small effective mass of electrons in InAs quantum is favorable to achieve high QCL performance in this spectral domain. Continuous wave operation at room temperature have been reported for InAs-based QCL emitting up to 18 μm [1].

LW-QCLs find application in chemical sensing of BTEX (benzene, toluene, ethylbenzene and xylene) which exhibit strong vibrational mode of the benzenic ring around 14-15 μm , or hydrocarbon compounds like propane. Chemical sensors based on laser spectroscopy using QCLs can fully leverage the performance of such sources to attain high detection sensitivity and selectivity. In these systems, high optical power and good beam quality are pre-requisites to fully exploit advantages of the laser spectroscopy. However, the optical power of LW-QCLs is fundamentally low, because of the small photon energy. For this reason, efficient use of the optical power generated in a QCL is crucial for LW spectroscopic applications.

Several strategies to enhance the available optical power have already been explored in different wavelength domains. Among them, the most successful are the Master Oscillator Power Amplifier (MOPA) device and tapered lasers. In the first, a laser oscillator is coupled to a pumped tapered section which behaves as a single pass amplifier. This way, the fundamental optical mode generated in the oscillator adiabatically expands in the tapered section, preserving its quality and enhancing its field amplitude. The drawback of such configuration lays in the device complexity since the oscillator and the amplifier parts must be individually optimized. The tapered laser, on the other side, combines the straight and the tapered parts in one oscillator. Clearly, one loses the capability of optimizing the individual sections with the advantage of having a two-terminal, less complex, device.

In both cases, the straight part serves to generate the fundamental optical mode in its narrow waveguide that does not support high-order transverse modes, while the tapered section provides its amplification. The second advantage consists in the narrower beam divergence along the slow axis coming from the wide tapered facet. Several taper geometries can be adopted, varying in terms of shape (linear, exponential, parabolic) and angle. In this work, we will refer to the taper angle as the angle formed between the straight section and the tapered section (half of the taper section aperture). Here we investigate on the performance and characteristics of long-wavelength tapered quantum cascade lasers. QCLs with linear tapers and angles of 1°, 2° and 3° were tested and compared with straight lasers in terms of electrical and optical characteristics and beam quality.

[*davide.pinto@tuwien.ac.at](mailto:davide.pinto@tuwien.ac.at); phone +39 334 799 9705

2. METHODOLOGY

2.1 Studied devices and fabrication

The studied InAs/AlSb QCLs were based on a design similar to that described in [2]. Cladding layers 3 μm thick made of S-doped InAs is used for optical confinement in the laser waveguide. The 3.5- μm -thick 45-period active region of the lasers is separated from the cladding layers by 3- μm -thick undoped InAs-spacers to reduce free carrier absorption. The structure was grown by molecular beam epitaxy in a Riber 412 machine.

Fabry-Pérot (FP) lasers were fabricated from this wafer by using classical photolithography steps. At first, deep mesas were formed via $\text{H}_3\text{PO}_4:\text{H}_2\text{O}_2:\text{H}_2\text{O}$ (2:1:2) wet chemical etching. Proper lithographic masks were employed to define the tapered geometry, with taper angles of 0° (straight laser), 1° , 2° and 3° and ridge width of 14 μm at the active zone. The lasers were insulated by hard-baking of a photoresist, preserving an opening on the top of the device to provide electrical contact. A metallization layer of Ti/Au/Cr/Au (20/200/30/200 nm) was deposited on top of the sample via e-beam evaporation. Finally, the device was mechanically polished and thinned down to a thickness of 200 μm and single lasers were cleaved. In Figure 1(a) a SEM micrograph of the straight-side facet can be seen. In (b), a top view of the tapered device after metallization is portrayed. Laser bars were then cleaved to form FP resonators 3.6 mm long with both facets left uncoated. Equal straight and tapered part length were chosen.

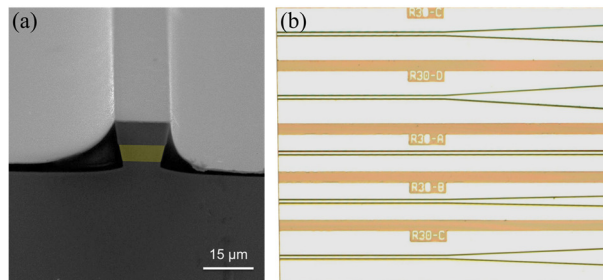


Figure 1. (a) Straight-side facet of the LW-QCL observed under scanning electron microscopy. The active zone corresponds to the yellow highlighted region. (b) Top view of tapered QCLs with angles of 0° , 1° , 2° and 3° indicated with A, B, C and D respectively.

The devices were individually soldered epi-side down with indium on AlN submounts. The lasers were tested at room temperature in pulsed operation with a pulse repetition rate of 12 kHz and a pulse duration of 330 ns, corresponding to a duty cycle of 0.4%. A square wave of 30 Hz was superimposed to provide higher sensitivity in combination with the slow the pyroelectric detectors employed for the characterization.

For the optical and spectral characterization, the laser was mounted in a temperature-stabilized system and the light was collected by using a parabolic gold mirror at 50 mm. A Bruker Vertex 70 FTIR spectrometer equipped with a pyroelectric DTGS detector was used for spectral characterizations of the fabricated devices.

Measurements of the far-field angular intensity distribution were performed by mounting the laser on a motorized rotation stage and collecting the light with a pre-amplified pyroelectric element, without the aid of focusing optical elements. The pyrodetector 1.3 mm in diameter was placed few centimeters apart from the front facet of the laser, providing an angular resolution of $\sim 1^\circ$. This way, the angular distribution of the far-field profile is directly recorded as a function of the stage rotation angle.

3. RESULTS

Voltage-current-power characteristics of the tapered lasers are presented in Figure 2(a). The threshold current scales with the taper angle as a consequence of the increased active volume. The tested devices exhibited threshold currents of 0.46, 1.14, 1.86 and 2.61 A, increasing with the taper angle. Such values correspond to threshold current densities of 1.25-1.3 kA/cm^2 . The optical power collected from the tapered facets is higher than for straight lasers. However, the reduced slow-axis divergence of tapered devices affects the collection efficiency, resulting in an apparent power enhancement that strongly exceeds the expected values, based on the bare increase of the active volume. The front facet in tapered devices can get up to 190 μm wide (3° -device), reducing the divergency of the output beam. For this reason, the collection efficiency is strongly improved for tapered lasers and the comparison of the light-current (LI) characteristics among such

lasers is not very informative. The non-linear behavior and the presence of kinks suggest that possible loss mechanisms take place, for instance the occurrence of sidelobes not efficiently collected by the parabolic mirror. For a fair comparison, we collected the light from the straight facet of the tapered lasers, in order to have the same beam divergency. Such analysis, presented in Figure 2 (b) demonstrated that the best average performances are obtained for a taper angle of 1°, while the 2°- and 3°-devices delivered less optical power than expected. This finding can be explained by assuming nonlinearities (thermal or electrical) occurring in the tapered device. A detailed analysis must be carried out to investigate the causes of such phenomenon.

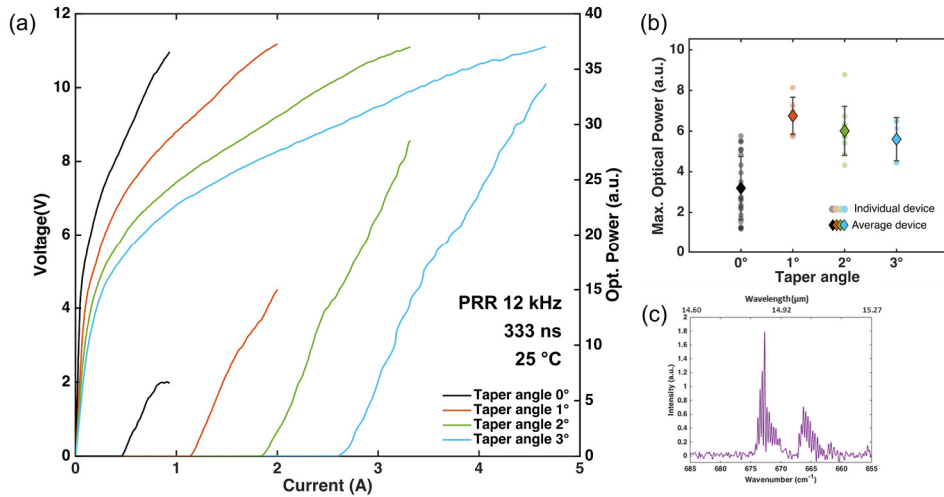


Figure 2. (a) Voltage-current-light characteristics of the tapered lasers, operated at a pulse repetition rate of 12 kHz, pulse duration of 300 ns and room temperature. (b) Maximum optical power output recorded from the straight facet for several devices. (c) Representative spectrum of a tapered LW-QCL.

The far-field angular intensity distribution along the slow-axis was analyzed by rotating the laser around its front facet in front of a pyroelectric detector. The far-field profiles for the four types of lasers are presented in Figure 3.

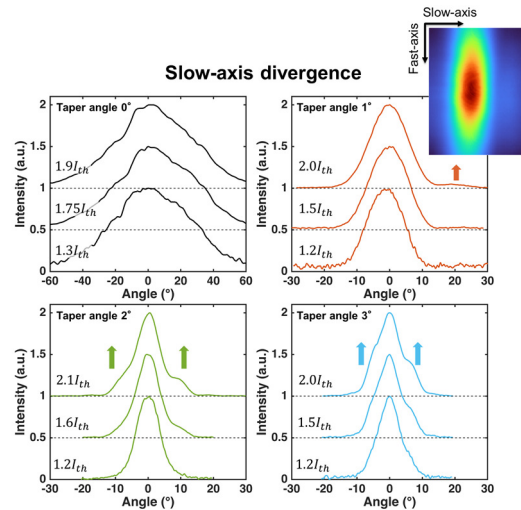


Figure 3. Far-field angular intensity distribution of the tapered lasers, measured for different operating currents. At higher currents, almost all the tapered lasers exhibit the occurrence of sidelobes, which degrades the beam quality. In the inset, an intensity map of the 1°-laser acquired with a microbolometer array camera is shown.

The study revealed a much narrower divergence angle for tapered devices, as it is expected for a wider emitting facet. For the estimation of the divergence angle and the beam quality, the second-order momentum of the angular intensity distribution and the M^2 factor were employed. The first is expressed as follows:

$$\sigma_{\theta}^2 = \frac{\int_{-\infty}^{+\infty} (\theta - \bar{\theta})^2 |E(\theta)|^2 d\theta}{\int_{-\infty}^{+\infty} |E(\theta)|^2 d\theta} \quad (1)$$

where $\bar{\theta}$ corresponds to the first-order momentum, while the latter is provided by:

$$M^2 = \frac{4\pi\sigma_0\sigma_{\theta}}{\lambda} \quad (2)$$

being $\sigma_0 = 0.181w$ the standard deviation of the near-field spatial intensity distribution, and w is the facet width. Straight lasers exhibit a wide distribution with a divergence half-angle that reaches 26° as it would be expected for a narrow waveguide. The intensity distribution does not change considerably with the injection current. On the other side, tapered devices show a much narrower divergence, with appearance of sidelobes as the operating current is increased. This causes a degradation of the beam quality and deviation from the gaussian distribution. A comprehensive summary of the results obtained is shown in Table 1. In the inset of Figure 3, a 2D image of the spatial intensity distribution of the 1° -tapered laser is shown, while operated at the highest current. The side lobe on the right is clearly recognizable. The fast-axis distribution confirms single transverse mode operation.

Table 1. Divergence angle and M^2 factor for different devices at low and high operating current.

Taper angle	σ_{θ} (low \rightarrow high current)	M^2 (low \rightarrow high current)
0°	$\sim 26^\circ$	≥ 1
1°	$5.6^\circ \rightarrow 6.5^\circ$	$1.07 \rightarrow 1.23$
2°	$3.7^\circ \rightarrow 5.0^\circ$	$1.31 \rightarrow 1.77$
3°	$4.0^\circ \rightarrow 5.0^\circ$	$2.00 \rightarrow 2.52$

4. CONCLUSIONS

We investigated the electrical and optical properties of tapered long-wavelength quantum cascade lasers with taper angles of 0° , 1° , 2° and 3° . In terms of electro-optical properties, the lasers present a threshold current which scales with the taper angle as a consequence of the larger active volume. All the devices showed similar threshold current densities of 1.25-1.3 kA/cm². For comparison of the optical performances, the light was collected from the straight side of all lasers in order to provide the same collection efficiency. The tapered devices delivered more optical power than straight lasers. In terms of beam quality, the 1° -devices exhibited a low divergency and highly gaussian beam, with the occurrence of sidelobes only at high operating currents. The analysis revealed that high-angle tapers produce less optical power than expected for the increased active volume, possibly due to nonlinearities occurring within the laser medium. The sidelobes occurring even at relatively low currents degraded the beam quality of high-angle tapers. To conclude, we demonstrated that tapered LW QCLs provide considerably higher optical powers compared with conventional straight ridge devices and excellent beam quality for small taper angles, 1° in our case.

REFERENCES

- [1] N.G. Van, Z. Loghmari, H. Philip, M. Bahriz, A.N. Baranov, and R. Teissier “Long wavelength ($\lambda > 17 \mu\text{m}$) distributed feedback quantum cascade lasers operating in a continuous wave at room temperature”, *Photonics*, 6, 31, 2019, doi:10.3390/photonics6010031
- [2] K. Kinjalk et al., “InAs-Based Quantum Cascade Lasers with Extremely Low Threshold,” *Photonics* 9(10), 747, MDPI AG (2022) [doi:10.3390/photonics9100747].